Available online at www.sciencedirect.com

ScienceDirect

Applied Geochemistry 22 (2007) 575–588

Applied Geochemistry

www.elsevier.com/locate/apgeochem

Stable chlorine isotopes in Phanerozoic evaporites

C.J. Eastoe [a,*], T.M. Peryt [b], Oleh Y. Petrychenko [c], D. Geisler-Cussey [d]

[a] Department of Geosciences, University of Arizona, Tucson, AZ 85721, USA
[b] Panstwowy Instytut Geologiczny, Rakowiecka 4, 00-975 Warsawa, Poland
[c] Institute of Geology and Geochemistry, National Academy of Sciences of Ukraine, Naukova 3a, 79053 Lviv, Ukraine
[d] Université de Pau et de Pays de l'Adour, Avenue de l'Université, 64000 Pau, France

Abstract

Modern seawater has a uniform δ^{37}Cl value (0.0‰), with an exception in the upper current of the Bosphorus (0.4‰). Marine halite ranging in age from Cambrian to Miocene has δ^{37}Cl values of 0.0 ± 0.9‰, with most of the data in the range 0.0 ± 0.5‰. Mean δ^{37}Cl values differ measurably between basins, with no evident relationship to basin size or to age. Smaller evaporite bodies have the largest δ^{37}Cl ranges. Potash facies halite has mean δ^{37}Cl values lower than those of halite facies salt in the East Siberia and Zechstein basins. The bulk δ^{37}Cl of bedded halite preserving sedimentary textures cannot be shifted measurably after deposition under plausible natural conditions. During the Phanerozoic, a detectable change in the δ^{37}Cl values of the oceans is unlikely as a result of Cl fluxes to and from the mantle and evaporites. In halite, the values of δ^{37}Cl that cannot be explained by fractionation occurring on crystallization are best explained by the addition of non-marine Cl with $\delta^{37}\text{Cl} \neq 0.0$‰ to evaporite brine.

1. Introduction

Certain aspects of the composition of seawater have varied through the Phanerozoic. The concentrations of K and Mg (Hardie, 1996), δ^{13}C (Veizer and Hoefs, 1976; Holser et al., 1988), δ^{34}S and δ^{18}O of SO_4^{2-}(Claypool et al., 1980; Holser et al., 1988) and ^{87}Sr/^{86}Sr (Peterman et al., 1970) all show cyclic variations driven by tectonics and, in the case of the C and S systems, by global-scale oxidation–reduction chemistry. In marine evaporites, the variations are reflected in the isotope composition of Ca sulfate minerals, in the mineralogy of potash facies salts, in the varied composition of primary fluid inclusions in primary-bedded halite (Kovalevich et al., 1998), and in the Br content of basal halites from unaltered marine evaporites (Siemann, 2003). The advent of high-precision measurements of δ^{37}Cl (Long et al., 1993) and the discovery of measurable Cl isotope fractionation between halite and its aqueous solution (Eggenkamp et al., 1995) suggest the possibility of looking for secular variation of δ^{37}Cl in marine evaporites.

At the outset, there is good reason to doubt the existence of large δ^{37}Cl variations in Phanerozoic seawater Cl^-. Chloride does not participate in

---

[*] Corresponding author.
E-mail addresses: eastoe@email.arizona.edu (C.J. Eastoe), tadeusz.peryt@pgi.gov.pl (T.M. Peryt), igggk@ah.ipm.lviv.ua (O.Y. Petrychenko), dominique.cussey@univ-pau.fr (D. Geisler-Cussey).

0883-2927/$ - see front matter © 2006 Elsevier Ltd. All rights reserved.
doi:10.1016/j.apgeochem.2006.12.012

oxidation–reduction chemistry in the oceans. All published δ^{37}Cl data (reviewed below) for marine evaporites fall within a narrow range, 0.0 ± 0.5‰, implying that fluxes between ocean and evaporite reservoirs should generate only small changes in δ^{37}Cl of the oceans. Mantle-to-crust fluxes are small relative to crustal reservoirs (Ito et al., 1983), suggesting minimal possibility for isotopic change from that source. Nonetheless, values of δ^{37}Cl outside the predicted range for halite formed from 0.0‰ marine Cl^- have been reported (Eastoe and Peryt, 1999).

In this paper, the authors present new δ^{37}Cl data for marine evaporites, and combine them with published data in a first attempt at constructing a marine Cl isotope record for the Phanerozoic. Data on the homogeneity of δ^{37}Cl in seawater are also reviewed. The potential causes of isotope fractionation in seawater and evaporites are discussed, and the following questions are addressed: (1) Are the data consistent with measured fractionation factors, in particular in the ranges of δ^{37}Cl in halite, and the relationship between potash and halite facies salts? (2) Is there evidence for the secular variation of δ^{37}Cl of the oceans? (3) Is there general or sporadic evidence for non-marine Cl^- input in putative marine evaporites? and (4) Is secondary (diapiric or open-space filling) salt fractionated with respect to primary (bedded) salt?

2. Previous work

Chlorine isotope data for marine evaporites have been published for the following examples: Zechstein basin, Netherlands, potash facies (Eggenkamp et al., 1995); Badenian basins of Poland, Slovakia and Ukraine, halite facies (Eastoe and Peryt, 1999); Palo Duro basin, Texas, halite facies (Eastoe et al., 1999) and Gulf of Mexico basin, halite and potash facies and diapiric halite (Eastoe et al., 2001). Eggenkamp et al. (1995) presented experimental data for Cl isotope fractionation between halite, sylvite and bischofite and their solutions at 22 °C. Eastoe et al. (1999) showed that δ^{37}Cl values of salts crystallized progressively from 0.0‰ seawater in the laboratory were consistent with the data of Eggenkamp et al. (1995). The existing δ^{37}Cl data for bedded halite and potash facies salts are consistent with the experimental data and a 0.0‰ ocean, except in the case of the Badenian basins, where Eastoe and Peryt (1999) detected episodic Cl^- inputs with distinctive non-zero δ^{37}Cl values.

3. New study areas

New data are available from the following areas. Sample locations are given in Table 1.

1. East Siberia. The salt deposits of Late Neoproterozoic to early Cambrian age in East Siberia cover an extensive area (ca. 2 million km^2) located to the NW of Lake Baikal. The thickness of the Vendian-Lower Cambrian succession is 2.0–2.5 km in the southern, western and central parts of the basin, and 1.3–1.5 km in the northeastern part. Paleogeographic data as well as a great total volume of Upper Vendian–Lower Cambrian evaporites of East Siberia are regarded as indications of a marine origin for the Siberian salt giant. It is characterized by the occurrence of 14 regional marker carbonate units and 15 salt units (Zharkov, 1984). Five major phases of salt deposition can be distinguished, in the Late Vendian (Danilovo) and Early Cambrian (Usolye, Belsk, Angara, and Litvintsevo) basins. The sample set represents halite facies, halite facies approaching sylvite saturation (recognized from fluid inclusion compositions – Petrychenko et al., 2005), and halite with potash salts from the Angara, Belsk and Usolye Series. The area of the Usolye salt basin reached 2 million km^2, and the average thickness of deposited salt is 200 m. Four major phases of halite precipitation occurred, and, episodically, K salts (carnallite and sylvite) were deposited in the upper part of stratigraphic section. The area of the Belsk salt basin was 1.3 million km^2, and the average thickness of salt deposits is 100 m. The Angara salt basin occupies 1.2 million km^2 and the salt thickness is 15–450 m (about 100 m on average; Zharkov, 1981). Potassium-bearing deposits occur in different stratigraphic levels; the total thickness of the potash salt complex (composed of carnallite and/or sylvinite) in the Nepa deposit attains 150 m (Mashovich et al., 1991).
2. Holbrook Basin, Arizona. Lower Permian salt occurs in the Supai formation in five depositional cycles separated by carbonate beds. Salt underlies about 9000 km^2 in the basin, with a maximum thickness of 180 m. Halite is muddy in general, indicating formation under sabkha conditions. Potash salts occur only in the upper 10–20 m of the fifth cycle (Rauzi, 2000).
3. Zechstein Basin, Poland and Germany. The Upper Permian (258–251 Ma) Zechstein Series consists of shale, carbonate, salt and anhydrite

Table 1
Data

No.	Formation	Locality	Borehole	Depth, m	δ^{37}Cl ‰	δ^{37}Cl ‰	Notes
East Siberia							
1	Angara	E Siberia	Nepa 3	463.5	0.1		Above sylvite
2	Angara	E Siberia	Nepa 3	469.0	−0.2		Above sylvite
3	Angara	E Siberia	Nepa 3	488.0	0.0		Above sylvite
4	Angara	E Siberia	Nepa 3	503.6	0.0		Above sylvite
5	Angara	E Siberia	Nepa 3	512.5	−0.2		Above sylvite
6	Angara	E Siberia	Nepa 3	542.8	−0.4		Above sylvite
7	Angara	E Siberia	Nepa 3	549.7	−0.1	−0.1	Above sylvite
8	Angara	E Siberia	Nepa 3	561.3	−0.4		Above sylvite
9	Angara	E Siberia	Nepa 3	578.1	−0.2		Above sylvite
10	Angara	E Siberia	Nepa 3	593.0	−0.5	−0.8	With sylvite
11	Angara	E Siberia	Nepa 3	620.1	−0.5		With sylvite
12	Angara	E Siberia	Nepa 3	675.8	−0.4		With sylvite
13	Angara	E Siberia	Bratsk 46	476.7	−0.2		Tr. diagen. K minerals
14	Angara	E Siberia	Bratsk 46	542.0	0.2		
15	Angara	E Siberia	Bratsk 46	850.0	−0.2		Close to KCl sat.
16	Angara	E Siberia	Bratsk 3s	1606.7	0.2		Tr. diagen. K minerals
17	Angara	E Siberia	Bratsk 3s	1815.6	0.4		Close to KCl sat.
18	Angara	E Siberia	Bratsk 47K	804.5	0.3		Close to KCl sat.
19	Angara	E Siberia	Bratsk 86	643.5	0.3		
20	Angara	E Siberia	Bratsk 86	776.5	−0.2		
21	Angara	E Siberia	Bratsk 86	1119.3	0.0		
22	Angara	E Siberia	Bratsk 28	873.2	−0.4	−0.2	Close to KCl sat.
23	Angara	E Siberia	Bratsk 57	400.0	−0.3		Close to KCl sat.
24	Angara	E Siberia	Bratsk 59K	723.0	0.3		
25	Angara	E Siberia	Bratsk 59K	918.0	0.2		
26	Angara	E Siberia	Bratsk 59K	928.0	−0.4		Close to KCl sat.
27	Usolye	E Siberia	Peledui 750	1431.4	0.0		Close to KCl sat.
28	Usolye	E Siberia	Taseyevo 54	873.4	−0.2	−0.2	Trace K minerals
29	Usolye	E Siberia	Shaman 20	1413.0	0.3		Close to KCl sat.
30	Usolye	E Siberia	Shaman 12	1394.0	0.2		
31	Usolye	E Siberia	Pokrovsk 141	1966.0	−0.4		
32	Usolye	E Siberia	Zayarsk 1	2209.5	−0.3	−0.4	With sylvite
33	Usolye	E Siberia	Zayarsk 1	2496.0	−0.9	−0.9	With sylvite
34	Usolye	E Siberia	Zayarsk 1	2517.0	−0.3	−0.4	
35	Belsk	E Siberia	Taseyevo 57	723.8	−0.5	−0.7	
36	Belsk	E Siberia	Taseyevo 57	905.5	−0.6		With sylvite
37	Belsk	E Siberia	Taseyevo 57	1403.0	−0.6		With carnallite
38	Belsk	E Siberia	Taseyevo 46	1023.0	−0.1		
39	Angara	E Siberia	Mirnyi 51D	478.0	−0.1		With carnallite
40	Angara	E Siberia	Mirnyi 51D	534.0	−0.3		With carnallite
41	Angara	E Siberia	Mirnyi 51D	536.0	1.0	0.9	With carnallite
42	Angara	E Siberia	Mirnyi 51D	581.0	0.0		With carnallite
43	Angara	E Siberia	Mirnyi 51D	813.0	0.4		
45	Belsk	E Siberia	Mirnyi 51D	1100.0	−0.3	−0.1	With sylvite
46	Belsk	E Siberia	Mirnyi 51D	1154.0	−0.3	−0.5	
47	Belsk	E Siberia	Mirnyi 51D	1176.0	−0.1	−0.2	
Holbrook Basin							
HBS-1	Supai	Arizona	AZPOT 11	363.6	−0.5	−0.2	Potash facies?
HBS-2	Supai	Arizona	AZPOT 11	367.3	−0.7	−0.4	Potash facies?
HBS-3	Supai	Arizona	AZPOT 11	379.4	−0.1		
HBS-4	Supai	Arizona	AZPOT 11	385.5	−0.5		
HBS-5	Supai	Arizona	AZPOT 11	397.6	−0.2		
HBS-6	Supai	Arizona	HPP55	214.8	−0.9		With sylvite
HBS-7	Supai	Arizona	HPP55	274.6	−0.1	0.1	

(*continued on next page*)

Table 1 (*continued*)

No.	Formation	Locality	Borehole	Depth, m	δ^{37}Cl ‰	δ^{37}Cl ‰	Notes
Zechstein 1							
1	Werra	Germany		1935.23	−0.1		
2	Werra	Germany		1936.44	0.2		
3	Werra	Germany		1936.99	0.2		
4	Werra	Germany		1937.78	0.0		
5	Werra	Germany		1938.68	−0.4		
6	Werra	Germany		1939.5	0.1		
Zechstein 1							
3A	Werra	N Poland	Zdrada IG3	804.3	0.2		
7	Werra	N Poland	Zdrada IG3	784.0	0.0	0.0	
3	Werra	N Poland	Zdrada IG6	941.6	−0.1		
12	Werra	N Poland	Zdrada IG6	904.3	0.2		
1	Werra	N Poland	Zdrada IG8	981.1	0.0		
4	Werra	N Poland	Zdrada IG8	947.7	0.2	0.4	
8	Werra	N Poland	Zdrada IG8	916.7	0.4		
12A	Werra	N Poland	Zdrada IG8	806.2	0.0		
16	Werra	N Poland	Zdrada IG8	846.6	0.2		
20	Werra	N Poland	Zdrada IG8	784.7	0.1		
Zechstein 2–3							
GW-1	Stassfurt	W Poland	Gorzów Wlkp. IG1	3022.9	0.0		
GW-2	Stassfurt	W Poland	Gorzów Wlkp. IG1	3013.8	−0.3		
GW-3	Stassfurt	W Poland	Gorzów Wlkp. IG1	3009.8	0.2		
GW-4	Stassfurt	W Poland	Gorzów Wlkp. IG1	2999.8	−0.5		
GW-5	Stassfurt	W Poland	Gorzów Wlkp. IG1	2973.0	−0.2		
GW-6	Stassfurt	W Poland	Gorzów Wlkp. IG1	2955.6	0.2		
GW-7	Stassfurt	W Poland	Gorzów Wlkp. IG1	2946.5	0.0		
GW-8	Stassfurt	W Poland	Gorzów Wlkp. IG1	2934.5	−0.1		
GW-9	Stassfurt	W Poland	Gorzów Wlkp. IG1	2828.2	0.3		
GW-10	Stassfurt	W Poland	Gorzów Wlkp. IG1	2923.0	0.2		
GW1-11	Leine	W Poland	Gorzów Wlkp. IG1	2853.6	0.3		
GW1-12	Leine	W Poland	Gorzów Wlkp. IG1	2840.1	0.0	0.2	
GW1-13	Leine	W Poland	Gorzów Wlkp. IG1	2828.0	0.2		
GW1-14	Leine	W Poland	Gorzów Wlkp. IG1	2823.9	0.1		
GW1-15	Leine	W Poland	Gorzów Wlkp. IG1	2811.4	0.1		
GW1-16	Leine	W Poland	Gorzów Wlkp. IG1	2789.5	−0.3	−0.3	
GW1-17	Leine	W Poland	Gorzów Wlkp. IG1	2773.4	0.0		
GW1-18	Leine	W Poland	Gorzów Wlkp. IG1	2761.9	0.1	0.3	
GW1-19	Leine	W Poland	Gorzów Wlkp. IG1	2750.4	0.3		
GW1-20	Leine	W Poland	Gorzów Wlkp. IG1	2743.4	0.0		
Paris Basin							
M1	Muschelkalk	Lorraine	Faulequemont	112.95	0.8	0.9	Bedded, dark
M2	Muschelkalk	Lorraine	Faulequemont	112.80	−0.3		Bedded, light
M3	Muschelkalk	Lorraine	Faulequemont	111.40	−0.5	−0.8	Displacive halite
M4	Muschelkalk	Lorraine	Faulequemont	111.10	0.1		Bedded
K1	Keuper	Lorraine	Gellenoncourt	291.25	−0.7	−0.6	Bedded, base of N
K2	Keuper	Lorraine	Gellenoncourt	289.95	0.2		Bedded
K3	Keuper	Lorraine	Gellenoncourt	289.38	−0.2		Bedded
K4	Keuper	Lorraine	Gellenoncourt	286.37	−0.1		Fissure filling
K5	Keuper	Lorraine	Gellenoncourt	286.13	0.1		Bedded
K6	Keuper	Lorraine	Gellenoncourt	285.75	0.0		Displacive halite
K7	Keuper	Lorraine	Gellenoncourt	282.12	0.2		Bedded, light
K8	Keuper	Lorraine	Gellenoncourt	274.05	0.0		Displacive halite
K9	Keuper	Lorraine	Gellenoncourt	274.00	−0.1	−0.2	Fibrous salt
K10	Keuper	Lorraine	Gellenoncourt	271.56	−0.4		Disrupted zone
K11	Keuper	Lorraine	Gellenoncourt	268.68	−0.3		Bedded, top of N
K12	Keuper	Lorraine	Gellenoncourt	267.90	−0.2		Displacive halite
K13	Keuper	Lorraine	Gellenoncourt	256.90	−0.5		Bedded, top of O
K14	Keuper	Lorraine	Gellenoncourt	245.42	−0.3		Bedded

Table 1 (*continued*)

No.	Formation	Locality	Borehole	Depth, m	δ^{37}Cl ‰	δ^{37}Cl ‰	Notes
K15	Keuper	Lorraine	Gellenoncourt	236.88	0.0		With polyhalite
K16	Keuper	Lorraine	Gellenoncourt	220.40	−0.1		With gl
K17	Keuper	Lorraine	Gellenoncourt	218.45	0.1		Fissure filling with gl
K18	Keuper	Lorraine	Gellenoncourt	217.20	0.0		Bedded with gl
K19	Keuper	Lorraine			−0.3		Fibrous salt
K20	Keuper	Lorraine			0.0		Cavity filling
Khorat Plateau							
KP1	Maha Sarakham	Thailand			0.9	0.9	
KP2	Maha Sarakham	Thailand			0.0		
KP3	Maha Sarakham	Thailand			−0.2		
KP4	Maha Sarakham	Thailand			0.1		
KP5	Maha Sarakham	Thailand			−0.2		
KP6	Maha Sarakham	Thailand			−0.9	−1.0	
KP7	Maha Sarakham	Thailand			−0.2		
KP8	Maha Sarakham	Thailand			−0.1		
KP9	Maha Sarakham	Thailand			−0.1		
KP10	Maha Sarakham	Thailand			−0.1		
KP11	Maha Sarakham	Thailand			0.0		
KP12	Maha Sarakham	Thailand			0.9	0.9	
KP13	Maha Sarakham	Thailand			0.0		
KP14	Maha Sarakham	Thailand			0.0		
KP15	Maha Sarakham	Thailand			−0.3		
KP16	Maha Sarakham	Thailand			−0.2		
KP17	Maha Sarakham	Thailand			0.1	−0.1	
KP18	Maha Sarakham	Thailand			−0.1		
KP19	Maha Sarakham	Thailand			−0.3		
KP20	Maha Sarakham	Thailand			−0.7		
KP21	Maha Sarakham	Thailand			0.2		
KP22	Maha Sarakham	Thailand			0.2		

Explanation: Second column of Cl isotope data gives repeat analyses. tr. diagen. = trace diagenetic, sat. = saturation, gl = glauberite.

beds. The primary thickness of the Zechstein series in the basinal areas is 1500–2000 m and the Zechstein salts cover an area of about 700,000 km^2 (Zharkov, 1984). Traditionally, four evaporitic cycles have been distinguished, and the youngest cycle can be further subdivided into five subcyclothems. Marine evaporites occur in the first three evaporitic cycles, and in the fourth cycle they are partly marine and partly continental in origin (Wagner and Peryt, 1997). For this study, the authors analyzed the samples of halite from the second (Stassfurt) and third (Leine) evaporitic cycles in a borehole (Gorzów Wielkopolski IG1) having a basin center location in west Poland, and from the first cycle (Werra) in 3 boreholes located in the peripheral evaporite platform and basin system in north Poland (Zdrada IG3, IG6 and IG8 – see Peryt et al., 1998, for a detailed geological setting).

4. Paris Basin, France. Thin evaporite beds about 235 Ma old, comprising 5 units with a maximum combined thickness of 25 m, occur within the Middle Triassic Muschelkalk stage (Hilly and Marchal, 1999). Sulfate and halite facies are present. Samples were obtained from a drill core at Faulquemont, Lorraine. The Muschelkalk is overlain by the Keuper stage, which contains thicker evaporite beds about 225 Ma old. Of eight separate salt units, three, termed N, O and P in ascending stratigraphic order, are thick enough to be of economic importance (Hilly and Marchal, 1999; Marchal, 1986). Each unit consists of multiple depositional sub-units up to a few meters thick of halite separated by thin argillaceous beds. The salt appears to have been deposited in a shallow basin of about 30,000 km^2, subject to frequent cycles of flooding and drying (Hilly et al., 1998). Samples for this study are from drill core from Gellenoncourt, Lorraine.
5. Khorat Plateau, Thailand. The Maha Sarakham evaporites of Late Cretaceous age, averaging 250 m thick, occur in a basin of about 160,000 km^2. Three cycles, comprising thick units

of anhydrite, halite and potash minerals, are present (El Tabakh et al., 1999; Hite and Japakasetr, 1979). The samples for this study represent the halite facies only.

4. Methods

Salt samples, in almost all cases 1–3 cm across, were dissolved in de-ionized water, and the Cl^- was precipitated as AgCl. CH_3Cl was prepared and measured according to the method of Long et al. (1993) on a modified VG602C mass spectrometer. Repeated measurements of the laboratory seawater standard indicated an analytical precision of 0.075‰ (1σ). Measurements are reported relative to the authors' laboratory standard, relative to which ISL354 is +0.05‰, and NBS 975 is +0.43‰ (Xiao et al., 2002). A day's measurements were accepted only after a satisfactory measurement on the laboratory standard. Laboratory intercomparisons between Arizona and Utrecht (unpublished) and Xining (Xiao et al., 2002) indicate satisfactory agreement.

5. Results

5.1. Seawater

Available evidence indicates that the present oceans are well-mixed with respect to Cl isotopes. Kaufmann (1984) and Eggenkamp et al. (1995) found no measurable variation in δ^{37}Cl in seawater. However, Xiao et al. (2002) reported an unexplained cluster of high δ^{37}Cl values (0.6 to 0.9‰) near a mid-ocean ridge in the Indian Ocean. In Fig. 1, further data are presented for seawater samples from around the world, relative to the results for the authors' laboratory standard, a seawater sample from San Diego, CA. All samples but one are consistent with the 0.0‰ value adopted for the laboratory standard. The exceptional sample, for which $\delta^{37}Cl = 0.4‰$, was taken from the surface current of the Bosphorus, about half way between the center of Istanbul and the Black Sea. The surface current consists of water from the upper, low-salinity layer of the Black Sea. Istanbul effluent is confined to the lower, denser current of Mediterranean seawater (0.0‰, on the indication of the sample from the Ionian Sea) entering the Black Sea through the Bosphorus.

5.2. Evaporites

The new data are listed with information on origin and mineralogy in Table 1. In Fig. 2, the data are presented as a series of histograms with classification. The authors have distinguished primary halite (including bedded and displaced halite) with no bittern salts, secondary halite (including open-space fillings and diapiric halite), and halite coexisting with potash and diagenetic sulfate minerals.

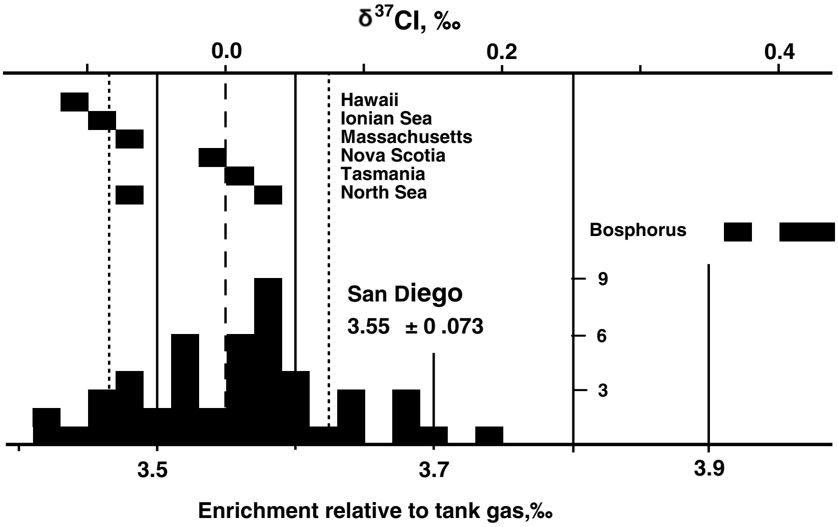

Fig. 1. New δ^{37}Cl data for seawater, shown as a frequency histogram relative to data for many repeated analyses of the authors'laboratory standard, seawater from San Diego.

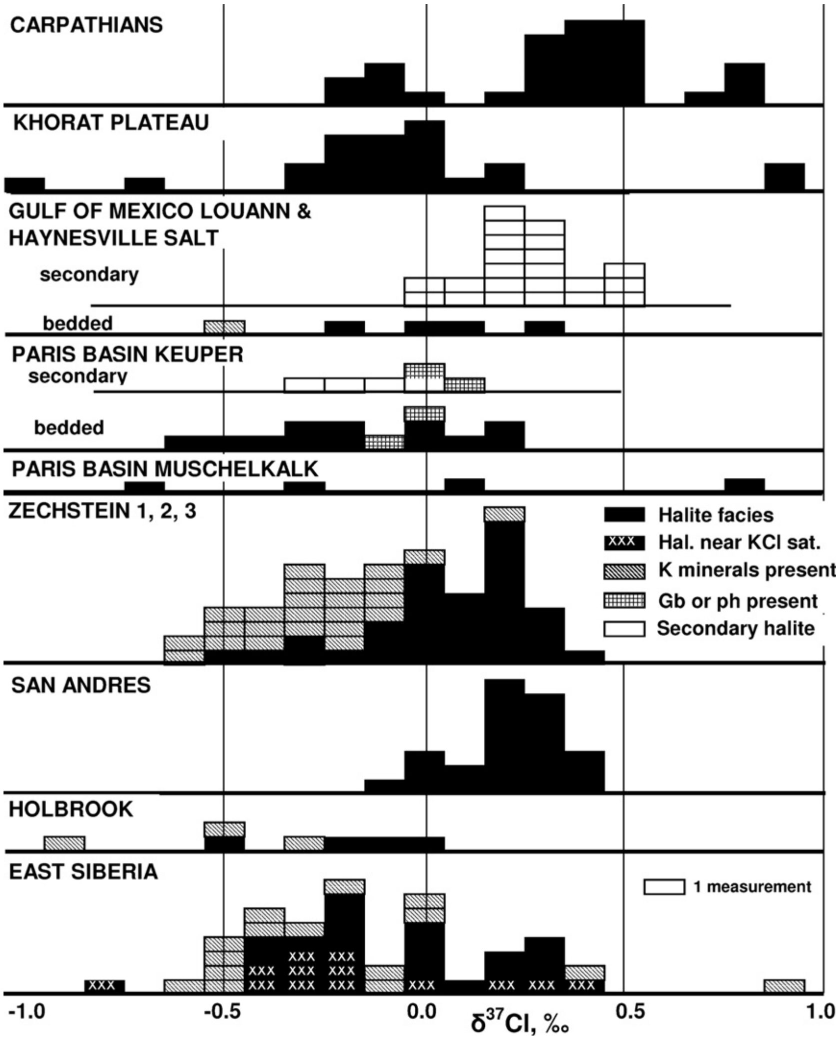

Fig. 2. Histograms of δ^{37}Cl of evaporite salt. Secondary salt is diapiric salt in the Gulf of Mexico Basin, and open-space filling salt in the Keuper. Gb = glauberite; ph = polyhalite. Data sources: Zechstein data include a set from Eggenkamp et al. (1995); San Andres: Eastoe et al. (1999); Gulf of Mexico: Eastoe et al. (2001); Carpathians: Eastoe and Peryt (1999); other data from this study.

In the case of the Cambrian evaporites of Siberia, a further distinction of halite approaching sylvite saturation is possible from fluid inclusion compositions (Petrychenko et al., 2005).

The δ^{37}Cl values of bedded halite span a range of −0.9 to +0.9‰, with most of the values falling between −0.5 and +0.5‰. Note that most of the more extreme measurements have been duplicated, and that such values are encountered in several of the sample sets. Bedded halite without bittern salts (indicated as halite facies in the figure) clearly differs isotopically between the sample sets. Fig. 3 shows the mean δ^{37}Cl values of bedded halite as a function of age for the larger data clusters which seem to form single populations. Outliers are omitted in the calculations. In the Carpathian Mts. data set, two populations can be justified on the basis of stratigraphy (Eastoe and Peryt, 1999). In the Siberia data set, most of the data are from a single formation (the Angara), and there is no apparent justification for distinguishing different populations. The mean of the Keuper data set takes into account the data for secondary halite, which is indistinguishable from the primary halite (see below).

Potash facies salt (mean δ^{37}Cl -0.30 ± 0.04‰) is isotopically lighter than halite facies salt (mean $+0.06 \pm 0.04$‰) in the Zechstein data set. In the Siberia data set, potash facies salt (mean -0.32 ± 0.06‰) is lighter than the halite facies salt (mean $+0.06 \pm 0.05$‰). Data from a single

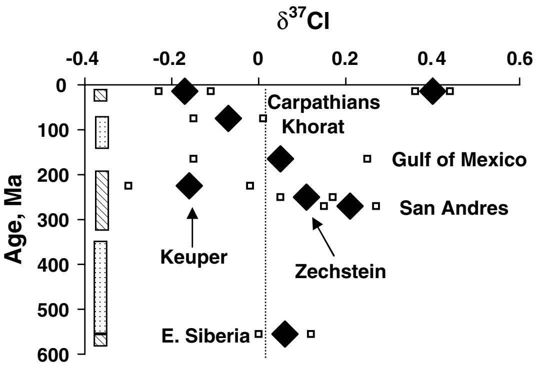

Fig. 3. Plot of mean δ^{37}Cl of halite facies salt as a function of age. Means (diamonds) are shown with error limits corresponding to two standard errors (squares). Dashed lines: limits of δ^{37}Cl of bulk halite formed from 0.0‰ brine. Rectangles along the time axis indicate times of low (dots) and high (stripes) Br content in basal marine halite, as calculated by Siemann (2003).

stratigraphic section in the Angara formation at Nepa illustrate the change in δ^{37}Cl between potash facies salt and overlying halite facies (Fig. 4). In this case, the overlying halite must represent a new cycle of evaporation; note that no values greater than 0.1‰ were measured. A halite of similar age in the Bratsk region yielded two clusters of δ^{37}Cl values, one being greater than 0.1‰.

5.3. Secondary effects

In the Gulf of Mexico Basin, diapiric halite has δ^{37}Cl values higher than those of bedded salt, for which few samples were available. Eastoe et al. (2001) suggested that solution during halokinesis might generate the high δ^{37}Cl values, which are too high to have formed from marine Cl$^-$ with δ^{37}Cl = 0‰. In the Paris Basin Keuper evaporites, on the other hand, secondary halite (open-space fillings with mean δ^{37}Cl = –0.11 ± 0.05) is indistinguishable from bedded halite (–0.13 ± 0.11‰). There is no evidence in this case of Cl isotope fractionation associated with dissolution and redeposition of halite. There is also no indication of fractionation associated with the formation of the diagenetic sulfate minerals glauberite and polyhalite.

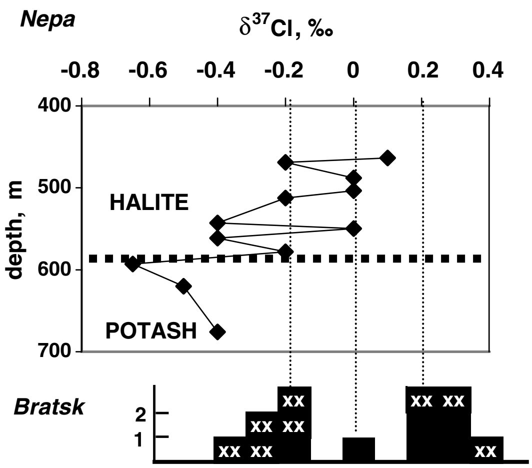

Fig. 4. Depth variation in δ^{37}Cl of salt in bedded salt from the Angara formation, Nepa, Eastern Siberia, compared with δ^{37}Cl values of salt from the Angara formation in the Bratsk region (shown as a frequency histogram; see Fig. 2 for legend).

6. Relationship between δ^{37}Cl values in halite and brine

6.1. Rayleigh distillation during halite formation

There are clear differences in the mean δ^{37}Cl values of bedded halite without bittern salts in the various sample sets used here. The means span a range of 0.6‰. Assuming that each sample set is representative of its salt body, and that post-depositional change is insignificant, it can be inferred that the mean δ^{37}Cl values of brines differed from basin to basin by the following argument.

The evolution of δ^{37}Cl in brine and halite in a salt-forming system can be modeled by Rayleigh distillation. Fig. 5a was constructed using the simplified form of the Rayleigh distillation equation, viz.

$$\delta - \delta_0 = \varepsilon \ln(f), \tag{1}$$

where δ_0 is the initial δ^{37}Cl value of the brine reservoir (given the value 0.0‰ in the figure), and δ is the δ^{37}Cl value of the brine corresponding to a residual Cl$^-$ fraction f in the brine. ε is δ^{37}Cl (halite)–δ^{37}Cl (brine), given a value of 0.26‰ (Eggenkamp et al., 1995). The δ^{37}Cl value of the accumulated halite formed up to a given value of f is

$$\delta_{\Sigma\text{hal}} = \delta + \varepsilon \ln(f)/(1 - f), \tag{2}$$

with values between 0.26 (f approaching 1) and 0.13‰ (f = 0.3, at the onset of bittern salt formation). If δ_0 is invariant, variation in f can therefore generate values of $\delta_{\Sigma\text{hal}}$ with a maximum range of 0.13‰. Little halite can form for values of f near 1, so that the range in practice is narrower, near 0.1‰. Clearly, variation in f at constant δ_0 cannot explain the 0.6‰ range of mean δ^{37}Cl in halite;

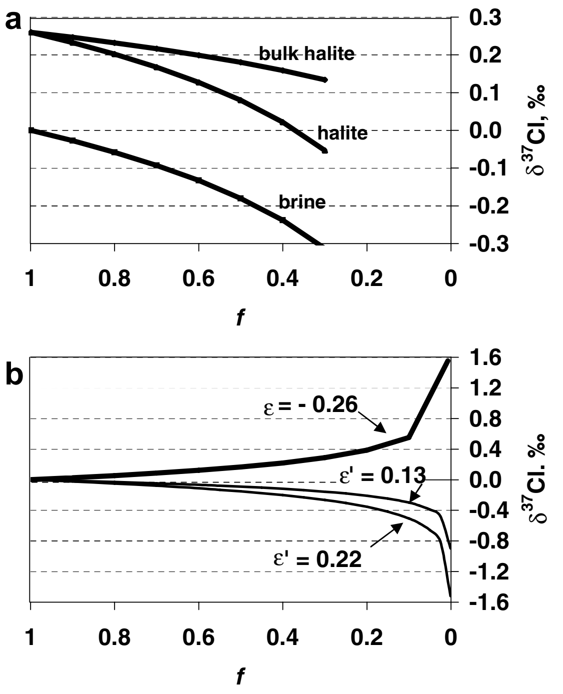

Fig. 5. (a) Rayleigh distillation of brine with initial $\delta^{37}Cl = 0.0‰$ as a function of *f*, residual fraction of Cl^- in the brine. Curves labeled "halite" and "brine" give coexisting $\delta^{37}Cl$ values at a particular value of *f*. The curve labeled "bulk halite" gives the bulk $\delta^{37}Cl$ value of halite accumulated up to a particular value of *f*. (b) Curve labeled $\varepsilon = -0.26$: evolution in $\delta^{37}Cl$ of salt in a diapir as a function of *f*, the residual fraction of salt remaining after incongruent dissolution. Curves labeled $\varepsilon' = 0.13$, 0.22: evolution of $\delta^{37}Cl$ of the oceans as a function of *f*, the residual fraction of salt remaining after extraction of halite. Initial $\delta^{37}Cl = 0.0‰$.

either variations in δ_0 or post-depositional shifts in $\delta^{37}Cl$ of halite are required. For $\delta_0 = 0.0‰$, bulk halite facies salt cannot have a negative value of $\delta^{37}Cl$.

6.2. Post-depositional effects

Congruent dissolution of halite accompanied by rapid removal of the solution, the situation most likely to occur around the edges of a halite body, leads to no shift in $\delta^{37}Cl$ of the residual halite. Incongruent dissolution – effectively dissolution with isotopic equilibration between salt and brine inside the halite body – leads to gradual increase in $\delta^{37}Cl$ of the residual halite if the brine is continuously expelled from the salt body (Eastoe et al., 2001). The curve labeled $\varepsilon = -0.26$ in Fig. 5b models such a increase using the Rayleigh equation. Measurable changes in $\delta^{37}Cl$ (0.15‰) are possible only after removal of about half of the halite. Such large losses are most unlikely under static conditions, particularly where primary textures are preserved, but may be possible as a result of halokinesis if the salt movement is accompanied by dissolution into pore fluid that is gradually cycled through the salt. Post-depositional effects cannot therefore explain the range of the $\delta^{37}Cl$ data in bedded halite.

The highest $\delta^{37}Cl$ values in diapiric salt from the Gulf of Mexico Basin are +0.5‰, higher than likely average $\delta^{37}Cl$ values for bedded halite in this basin by 0.3 to 0.5‰. Such a shift requires the removal of 60–90% of original halite (Fig. 5b), which may be reasonable. Davison et al. (1996) noted that diapir volumes in the North Sea basin are on the order of one-tenth of the volume of the likely source of bedded halite. Warren (1999) interpreted this discrepancy as the evidence of the loss of halite by dissolution. Buchanan et al. (1996) on the other hand saw no evidence of halite loss by dissolution in balanced sections including diapiric halite. Diapiric movement of single salt masses may continue for hundreds of millions of years (e.g. Burliga, 1996), giving ample opportunity for slow cycling of pore fluid through the salt.

7. Mechanisms of change of $\delta^{37}Cl$ in brine

7.1. Non-marine chloride sources

Evaporite formation commonly occurs in basins with highly restricted connections to the open seas, and are likely to receive, at least episodically, water and solute of non-marine derivation (Hardie, 1984). The sample from the Bosphorus is instructive because it indicates the possibility of non-zero values of $\delta^{37}Cl$ in isolated basins subject to the episodic input of seawater. The Miocene basins in which evaporites formed in front of the advancing Carpathian thrust belt were tectonically analogous to the Black Sea. The Miocene evaporites have $\delta^{37}Cl$ values indicating the addition of high- $\delta^{37}Cl$ non-marine Cl^- to any 0.0 ‰ marine Cl^- (Eastoe and Peryt, 1999).

Whether non-marine Cl^- can constitute a detectable fraction of Cl^- in a marine evaporite basin may depend on the basin geometry. Warren (1999) distinguished three environments in which marine evaporites form: (1) extensive subaerial mudflats to which seawater is supplied by storm surges; (2) salterns, shallow coastal basins subject to desiccation and fed by seawater seepage through the bars that separate them from the open sea; and (3) basins in which evaporite minerals are deposited in relatively deep standing brine that is replenished by the seepage of seawater. All seem equally likely to receive a mixture of marine and non-marine Cl^-. Smaller basins are more prone to shifts of $\delta^{37}Cl$ away from the $\delta^{37}Cl$ value of seawater as a result of non-marine inputs. Very large salt deposits should reflect $\delta^{37}Cl$ of seawater more closely because only a very large source of Cl^- (the ocean) is capable of sufficient supply. In the case of mudflats, the diffusion of Cl^- across concentration gradients in the subsurface might affect the isotopic composition of displacive halite.

7.2. Evolution of $\delta^{37}Cl$ in seawater: Cl fluxes to and from the mantle

Table 2 is a summary of data on the geochemical cycle of Cl. Ito et al. (1983) considered fluxes from the mantle to the ocean + crust (at hot spot and mid-ocean ridge volcanoes) to be balanced, within the error of their estimates, by the return subduction flux minus recycled Cl^- emergent in island arc volcanoes. The $\delta^{37}Cl$ of ocean Cl^- might change with time if a flux of juvenile Cl of distinctive $\delta^{37}Cl$ is constantly supplied. From Table 2, the ratio of the surface Cl reservoirs (crust + ocean) to the annual mantle-derived Cl flux through mid-ocean ridges and hot spots is about 10^{10}. Suppose that the mantle-derived flux is constant over t years and has $\delta^{37}Cl = M$. The $\delta^{37}Cl$ value, δ, of the surface reservoirs t years ago is given by the following mass balance equation:

$$\begin{array}{lll} \delta(1-10^{-10}t) & +M\times 10^{-10}t & = 0\times 1 \\ \text{initial} & +\text{flux} & =\text{final} \end{array} \qquad (3)$$

For $t = 5\times10^{8}$ a, $\delta = -0.053$ M. For $M = -1‰$, (considered a likely value by Sharp et al. (2005); and consistent with carbonatite $\delta^{37}Cl$ data of Eggenkamp and Koster van Groos (1997)), $\delta = 0.053$, indistinguishable from the present value. For $M = 5‰$ (Magenheim et al., 1995), $\delta = -0.26‰$, just detectable with available precision. If the mantle $\delta^{37}Cl$ is indeed –1‰, changes in $\delta^{37}Cl$ in surface reservoirs would be detectable only for time scales on the order of 10^9 a. Likewise, the return flux, which must remove Cl of $\delta^{37}Cl$ close

Table 2
The geochemical cycle of chlorine

A. Principal reservoirs (kg Cl)

Reservoir	Schilling et al. (1978)	Smith (1981)
Sediments	1.84×10^{19}	1.8×10^{19}
Ocean	2.71×10^{19} (equiv. to 2.0×10^{7} km^3)	2.7×10^{19}
Earth	1.5×10^{20}	2.7×10^{20}

B. Annual fluxes to and from surface reservoirs (kg Cl)

Type	Schilling et al. (1978)	Anderson (1974)	Ito et al. (1983)
Mid-ocean ridges	1.92×10^{9}	4.2×10^{9}	2.7×10^{9} (+2.7/–1.3)
Hotspots	1.29×10^{9}		1.3×10^{9} (+1.3/–1.2)
Island Arcs		3×10^{9}	4.5×10^{9} (+9.5/–4.3)
Alteration of ocean crust			$(-2.9\pm1.5)\times10^{9}$
Subduction of sediments			$(-3.2\pm1.0)\times10^{9}$
Total without subduction of sediments			5.6×10^{9} (+15.0/–8.3)
Total with subduction of sediments			2.4×10^{9} (+16.0/–9.3)

C. Volume of halite in certain evaporites, 10^5 km^3

Example	Volume	% of ocean salt	Example	Volume	% of ocean salt
Cambrian, Siberia	5.9	3	Permian, US midcontinent	0.63	0.3
Cambrian, Iran and Pakistan	5.9	3	Permian, Holbrook	0.004	0.002
Devonian, Siberia	0.14	0.07	Jurassic, Gulf of Mexico	16	8
Devonian, Eastern Europe	0.69	0.5	Cretaceous, Khorat	0.2	0.1
Devonian, Western Canada	0.62	0.3			
Permian, Eastern Europe	10.2	5			
Permian, Zechstein	1.5	0.8			

Sources: Paleozoic: minimum estimates, Zharkov (1981, 1984); Gulf of Mexico: Salvador (1991); Khorat: from basin area of Hite and to 0.0‰, is unlikely to change δ^{37}Cl of the oceans detectably during the Phanerozoic.

7.3. Evolution of δ^{37}Cl of seawater: Cl fluxes to and from evaporites

The formation of evaporites leads to episodic large fluxes of Cl from the ocean to the evaporite reservoir (Zharkov, 1981; Floegel et al., 2005), countered by the erosion of evaporites and the return of Cl^- to seawater. In the long term, the isotope effects of the fluxes should cancel each other if seawater δ^{37}Cl remains constant. The distribution of δ^{37}Cl in Phanerozoic evaporites sampled to date appears to have a mean δ^{37}Cl near 0.0‰ (Fig. 2), suggesting a long-term return flux δ^{37}Cl near 0.0‰. Temporary changes in the δ^{37}Cl of marine Cl^- might occur at times of giant evaporite formation, out of balance with the return flux. The preeminent time of salt extraction from the oceans was during the Jurassic and Cretaceous when halite was deposited in the rifts that were to become the Gulf of Mexico and the Atlantic Ocean. Halite still present in the Gulf of Mexico alone surpasses all other examples in Table 2 in volume. Floegel et al. (2005) suggested that salt extraction from the oceans has caused a decrease in salinity from about 50‰ in the early Paleozoic to the present value of about 34.7‰, with the most rapid change occurring during the Mesozoic.

Evaporites seldom form by total desiccation of a batch of brine to yield the complete the classic sequence of carbonate, gypsum, halite and bittern salts; the process may be interrupted at any point by dilution or by the removal of residual brine, or may be sustained in a single facies if seawater input is appropriately balanced by evaporative water loss. If evaporite formation always proceeded to a complete desiccation, there could be no consequent change in δ^{37}Cl of the oceans. Long-term change would require the separation of halite (sequestered in the crust) from bittern brine (recycled rapidly to the oceans). In fact, large volumes of halite appear to form without corresponding volumes of bittern salts (e.g. in the Gulf of Mexico basin; Salvador, 1991), so that the deposition of halite could potentially cause changes in δ^{37}Cl of the oceans.

Let us suppose that there is a value of f (see Eq. (1)) characteristic of halite formation in general. The evolution of seawater δ^{37}Cl as a consequence of halite deposition can then be modeled as a Rayleigh distillation using an effective fractionation ε' equal to the $\delta_{\Sigma hal}$ value corresponding to the characteristic value of f (Eq. (2), Fig. 5a). Two cases are shown in Fig. 5b. It is necessary to remove at least 70% of the salt in the oceans to generate a decrease of 0.3‰ in δ^{37}Cl in the oceans. There is no evidence that such an amount of salt has ever been deposited, at short or long time scale. At present, evaporites may contain an amount of salt equal to 30% of the present oceanic salt inventory (Holland, 1984, p. 464), or 43% (equivalent to 30% of the early Paleozoic inventory) if the salinity changes suggested by Floegel et al. (2005) are correct. This estimate is broadly consonant with the sizes of evaporites in individual basins, which do not appear to exceed 8% of the present oceanic inventory (Table 2). A rapid formation of giant halite evaporites such as the Louann Salt is therefore incapable of fractionating the residual Cl^- in the oceans measurably, even if the original size of the evaporite was twice that of the existing body.

7.4. Implications for δ^{37}Cl of evaporites

The value of δ^{37}Cl of the oceans is unlikely to have changed measurably during the Phanerozoic as a result of additions from the mantle, or of fluxes related to the evaporite cycle. Additions of non-marine, non-0.0‰ Cl^- are the best explanation of the observed variation in mean δ^{37}Cl of the larger data sets. This interpretation is supported by several other lines of reasoning. First, the values of δ^{37}Cl vary over short time intervals, as in Miocene salt at Wieliczka, where the data require influxes of high-δ^{37}Cl and low-δ^{37}Cl non-marine brines (Eastoe and Peryt, 1999). The contrast between Cambrian salt sections of similar age in the Nepa and Bratsk areas (Fig. 4) is a second example. Second, the extreme δ^{37}Cl values (near +1 or −1‰) have been encountered in halite in five of the basins studied here. Such values are clearly not rare, and reflect the localized dominance of fractionated Cl^- sources. Third, it is smaller salt bodies, viz. Carpathians, Khorat, Muschelkalk, Holbrook and San Andres, that show the most extreme variations in δ^{37}Cl. Fourth, variations in the data set appear to be random in time. A change in δ^{37}Cl of the oceans would be unidirectional, if related to gradual removal of Cl from the mantle, or cyclic on a scale of 100–200 Ma if related to mid-ocean ridge processes, as appears to be the case for variations in seawater chemistry (Hardie, 1996). The possibility of tectonic influence on δ^{37}Cl in brine merits more detailed discussion.

8. Tectonic influences

8.1. Ocean-scale variations

Siemann's (2003) data for Br in basal, unaltered marine halite make a strong independent case for the relationship between ocean major-ion chemistry and the rate of generation of ocean crust (Hardie, 1996). In Fig. 3, there is no apparent relationship between bulk δ^{37}Cl and basal Br content. The partition coefficient for Br^- between brine and halite depends on ion activities that are strongly influenced by the relative amounts of other ions such as SO_4^{2-}, K^+ and Mg^{2+}. Whether similar controls exist in relation to the partitioning of Cl isotopes remains untested in the laboratory. The lack of relationship between Br and δ^{37}Cl suggests that any such effect is not a primary influence on the isotope data.

8.2. Tectonic environment of basins

R. Sarg (pers. comm.) has observed that the basins studied here could be grouped as syn- to post-orogenic (Carpathians, Zechstein, San Andres) as opposed to syn- to post-rift (Gulf of Mexico, Paris Basin). Bulk bedded halite in the former set of basins has higher bulk δ^{37}Cl values than in the latter set (Fig. 3). To the former set can be added the Black Sea. It could be argued that the latter set belongs to a broader set of non-orogenic basins, in which case the Khorat, Holbrook and East Siberia basins, all with low bulk δ^{37}Cl values, can be added. In the Khorat and East Siberia basins, stable shelf sedimentation succeeded rifting that had occurred tens of millions of years earlier (El Tabakh et al., 1999; Ulmishek, 2001). The Holbrook basin forms part of a continental shelf succession little affected by orogeny (Dickinson, 1989). The salt in the Paris, Khorat, Holbrook and East Siberia basins did not fill rifts *per se*, but it was clearly not deposited in a compressional or post-compressional tectonic setting. Note, however, the negative δ^{37}Cl values of one episode of salt formation at Wieliczka (Eastoe and Peryt, 1999), in a setting that is clearly compressional, and a bracket of high δ^{37}Cl values at Bratsk, Eastern Siberia (Fig. 4). The evaluation of an association of higher bulk δ^{37}Cl values with compressional tectonics must wait for future research.

9. Conclusions

1. Detectable variations in δ^{37}Cl of seawater are improbable during the Phanerozoic, on the basis of current knowledge of the geochemical cycle of Cl and the δ^{37}Cl values of major reservoirs.
2. The values of δ^{37}Cl of putative marine halite lie in the range $0.0 \pm 0.9‰$, with most data in the range $0.0 \pm 0.5‰$.
3. Bulk δ^{37}Cl data for halite facies salt ranges more widely than can be explained by the formation from seawater Cl^- with $\delta^{37}Cl = 0.0‰$. The data are best explained by the addition of Cl^- of non-0.0‰ δ^{37}Cl to evaporite brine. This effect appears to be common.
4. Potash facies salt is in general (but not in detail in all cases) of lower δ^{37}Cl than halite facies salt, consistent with laboratory experiments.
5. Available data indicate that modern seawater has a uniform δ^{37}Cl value of 0.0‰, except for Black Sea surface water, which has $\delta^{37}Cl = 0.4‰$.
6. Halokinesis leads to increases in δ^{37}Cl of salt in diapirs in the Gulf of Mexico basin, but syn-sedimentary formation of secondary salt in the Keuper formation has not given rise to changes in δ^{37}Cl of salt.

Acknowledgements

The authors thank John Warren, Christian Strohmenger and the Arizona Geological Survey for samples from the Khorat Plateau, Zechstein1 and the Holbrook basin, respectively. They thank Yorgos Moussouris, Edwin Roedder, Steven Slaff and Hans Eggenkamp for providing seawater samples from distant places. The Laboratory of Isotope Geochemistry at the University of Arizona provided the analyses. The authors also thank R.Sarg, M.Siemann and an anonymous reviewer for their discussion.

References

Anderson, A.T., 1974. Chlorine, sulfur and water in the magmas and oceans. Bull. Geol. Soc. Am. 85, 1485–1492.

Buchanan, P.G., Bishop, D.J., Hood, D.N., 1996. Development of salt-related structures in the central North Sea: results from section balancing. In: Alsop, G.I., Blundell, D.J., Davison, I. (Eds.), Salt Tectonics. The Geological Society, London, pp. 11–128.

Burliga, S., 1996. Kinematics within the Kłodawa salt diapir, central Poland. In: Alsop, G.I., Blundell, D.J., Davison, I. (Eds.), Salt Tectonics. The Geological Society, London, pp. 1–21.

Claypool, G.E., Holser, W.T., Kaplan, I.R., Sakai, H., Zak, I., 1980. The age curves of sulfur and oxygen isotopes in marine sulfate and their mutual interpretation. Chem. Geol. 28, 199–260.

Davison, I., Alsop, G.I., Blundell, D.J., 1996. Salt tectonics: some aspects of deformation mechanics. In: Alsop, G.I., Blundell, D.J., Davison, I. (Eds.), Salt Tectonics. The Geological Society, London, pp. 1–10.

Dickinson, W.R., 1989. The tectonic setting of Arizona through geologic time. In: Jenney, J.P., Reynolds, S.J. (Eds.), Geologic evolution of Arizona. Arizona Geol. Soc. Dig. 17, pp. 1–16.

Eastoe, C.J., Peryt, T., 1999. Multiple sources of chloride in Badenian evaporites, Carpathian Mountains: stable chlorine isotope evidence. Terra Nova 11, 118–123.

Eastoe, C.J., Long, A., Knauth, L.P., 1999. Stable chlorine isotopes in the Palo Duro Basin, Texas: evidence for preservation of Permian evaporite brines. Geochim. Cosmochim. Acta 63, 1375–1382.

Eastoe, C.J., Long, A., Land, L.S., Kyle, J.R., 2001. Stable chlorine isotopes in halite and brine from the Gulf Coast Basin: brine genesis. Chem. Geol. 176, 343–360.

Eggenkamp, H.G.M., Koster van Groos, A.F., 1997. Chlorine stable isotopes in carbonatites: evidence for isotopic heterogeneity of the mantle. Chem. Geol. 140, 137–143.

Eggenkamp, H.G.M., Kreulen, R., Koster van Groos, A.F., 1995. Chlorine stable isotope fractionation in evaporites. Geochim. Cosmochim. Acta 59, 5169–5175.

El Tabakh, M., Utha-Aroon, C., Schreiber, B.C., 1999. Sedimentology of the Maha Sarakham evaporites in the Khorat Plateau of northeastern Thailand. Sediment. Geol. 123, 31–62.

Floegel, S., Hay, W.W., Migdisov, A., Balukhovsky, A.N., Wold, C.N., Soeding, E., 2005. Evaporites and the salinity of the ocean during the Phanerozoic: implications for climate, ocean circulation and life. Eos Trans. AGU, 86(52), Fall Meet. Suppl, Abstr. PP51A-0581.

Hardie, L.A., 1984. Evaporites: marine or non-marine? Am. J. Sci. 284, 193–240.

Hardie, L.A., 1996. Secular variation in seawater chemistry: an explanation for the coupled secular variation in the mineralogies of marine limestones and potash evaporites over the past 600 m.y. Geology 24, 279–283.

Hilly, J., Marchal, C., 1999. Les gisements évaporatiques de Lorraine. Bull. Inf. Géol. Bass. Paris 36, 20–24.

Hilly, J., Marchal, C., Buffet, A., 1998. La série évaporitique keupériennede Lorraine-Champaigne (France). Analyse et implications génétiques des discontinuités sédimentaires. Compt. Rend. Acad. Sci. Paris, Sci. de la Terre et des Planètes 326, 427–432.

Hite, R.J., Japakasetr, T., 1979. Potash deposits of the Khorat Plateau, Thailand and Laos. Econ. Geol. 74, 448–458.

Holland, H.D., 1984. The Chemical Evolution of the Atmosphere and Oceans. Princeton University Press, Princeton.

Holser, W.T., Schidlowski, M., Mackenzie, F.T., Maynard, J.B., 1988. Biogeochemical cycles of carbon and sulfur. In: Gregor, C.B., Garrels, R.M., Mackenzie, F.T., Maynard, J.B. (Eds.), Chemical Cycles in the Evolution of the Earth. Wiley, New York, pp. 105–174.

Ito, E., Harris, D.M., Anderson, A.T., 1983. Alteration of ocean crust and geologic recycling of chlorine and seawater. Geochim. Cosmochim. Acta 47, 1613–1624.

Kaufmann, R.S., 1984. Chlorine in ground water: stable isotope distribution. Unpubl. Ph.D. Diss., Univ. Arizona, Tucson.

Kovalevich, V.M., Peryt, T.M., Petrichenko, O.I., 1998. Secular variation in seawater chemistry during the Phanerozoic as indicated by brine inclusions in halite. J. Geol. 106, 695–712.

Long, A., Eastoe, C.J., Kaufmann, R.S., Martin, J.G., Wirt, L., Finley, J.B., 1993. High-precision measurement of chlorine stable isotope ratios. Geochim. Cosmochim. Acta 57, 2907–2912.

Magenheim, A.J., Spivack, A.J., Michael, P.J., Gieskes, J.M., 1995. Chlorine stable isotope composition of the oceanic crust: implications for earth's distribution of chlorine. Earth Planet. Sci. Lett. 131, 427–432.

Marchal, C., 1986. Le sel: marqueur stratigraphique et reflet de l'évolution structurale d'un bassin à partir de corrélations diagraphiques entre les séries keupériennes de l'Europe du NW. Compt. Rend. Acad. Sci. Paris 303, 1135–1140.

Mashovich, Y.G., Drugov, G.M., Galkin, G.A., Andreev, P.Y., 1991. Osobennosti stroyenia i uslovia obrazovania solenosnykh otlozheniy kembria na yuge Sibirskoy platformy. In: Zharkov, M.A., Merzlakov, G.A. (Eds.), Problemy Morskogo i Kontinentalnogo Galogeneza. Novosibirsk, Nauka, pp. 160–169.

Peryt, T.M., Pierre, C., Gryniv, S.P., 1998. Origin of polyhalite deposits in the Zechstein (Upper Permian) Zdrada Platform (northern Poland). Sedimentology 45, 565–578.

Peterman, Z.E., Hedge, C.E., Tourtelot, H.A., 1970. Isotopic composition of strontium in seawater throughout Phanerozoic time. Geochim. Cosmochim. Acta 34, 105–120.

Petrychenko, O.Y., Peryt, T.M., Chechel, E.I., 2005. Early Cambrian seawater chemistry from fluid inclusions in halite from Siberian evaporites. Chem. Geol. 219, 149–161.

Rauzi, S.L., 2000, Permian salt in the Holbrook basin, Arizona. Arizona Geol. Surv. Open-file Rep. 00–03.

Salvador, A., 1991. Triassic-Jurassic. In: Salvador, A., (Ed.), The Gulf of Mexico Basin: Boulder, Colorado, Geol. Soc. America, The Geology of North America, vol. J, pp. 131–180.

Schilling, J.-G., Unni, C.K., Bender, M.L., 1978. Origin of chlorine and bromine in the oceans. Nature 273, 631–636.

Sharp, Z.D., Barnes, J.D., Brearley, A.J., Chaussidon, M., Van Zuilen, M., 2005, The global chlorine cycle over the last 3.7 Ga; chlorine isotope constraints. Geol. Soc. Am. Ann. Meeting, Abstr. with Prog, Abstr. No. 147-2.

Siemann, M.G., 2003. Extensive and rapid changes in seawater chemistry during the Phanerozoic: evidence from Br contents in basal halite. Terra Nova 15, 243–248.

Smith, J.V., 1981. Halogen and phosphorus storage in the earth. Nature 289, 762–765.

Ulmishek, G.F., 2001. Petroleum geology of the Nepa-Botuoba high, Angara-Lena terrace, and Cis-Patom foredeep, southeastern Siberian Craton, Russia. US Geol. Surv. Bull. 2201-C.

Veizer, J., Hoefs, J., 1976. The nature of O^{18}/O^{16} and C^{13}/C^{12} secular trends in sedimentary carbonate rocks. Geochim. Cosmochim. Acta 40, 1387–1395.

Wagner, R., Peryt, T.M., 1997. Possibility of sequence stratigraphic subdivision of the Zechstein in the Polish Basin. Geol. Quart. 41, 457–474.

Warren, J., 1999. Evaporites: their evolution and economics. Blackwell, Oxford.

Xiao, Yingkai, Zhou, Yinming, Wang, Qingzhong, Wei, Haizhen, Liu, Weiguo, Eastoe, C.J., 2002. A secondary isotopic reference material of chlorine from selected seawater. Chem. Geol. 182, 655–661.

Zharkov, M.A., 1981. History of Paleozoic Salt Accumulation. Springer Verlag, Berlin.

Zharkov, M.A., 1984. Paleozoic Salt Bearing Formations of the World. Springer Verlag, Berlin.